Current Biology 23, 2443–2451, December 16, 2013 ©2013 Elsevier Ltd All rights reserved http://dx.doi.org/10.1016/j.cub.2013.09.062

Article

CHD4 Is a RanGTP-Dependent MAP that Stabilizes Microtubules and Regulates Bipolar Spindle Formation

Hideki Yokoyama,[1,*] Konstantinos Nakos,[2] Rachel Santarella-Mellwig,[1] Sofia Rybina,[1] Jeroen Krijgsveld,[1] Maria D. Koffa,[2,*] and Iain W. Mattaj[1]
[1]European Molecular Biology Laboratory, Meyerhofstrasse 1, Heidelberg 69117, Germany
[2]Department of Molecular Biology and Genetics, Democritus University of Thrace, University Campus Dragana, Alexandroupolis 68100, Greece

Summary

Background: Production of the GTP-bound form of the Ran GTPase (RanGTP) around chromosomes induces spindle assembly by activating nuclear localization signal (NLS)-containing proteins. Several NLS proteins have been identified as spindle assembly factors, but the complexity of the process led us to search for additional proteins with distinct roles in spindle assembly.
Results: We identify a chromatin-remodeling ATPase, CHD4, as a RanGTP-dependent microtubule (MT)-associated protein (MAP). MT binding occurs via the region containing an NLS and chromatin-binding domains. In *Xenopus* egg extracts and cultured cells, CHD4 largely dissociates from mitotic chromosomes and partially localizes to the spindle. Immunodepletion of CHD4 from egg extracts significantly reduces the quantity of MTs produced around chromatin and prevents spindle assembly. CHD4 RNAi in both HeLa and *Drosophila* S2 cells induces defects in spindle assembly and chromosome alignment in early mitosis, leading to chromosome missegregation. Further analysis in egg extracts and in HeLa cells reveals that CHD4 is a RanGTP-dependent MT stabilizer. Moreover, the CHD4-containing NuRD complex promotes organization of MTs into bipolar spindles in egg extracts. Importantly, this function of CHD4 is independent of chromatin remodeling.
Conclusions: Our results uncover a new role for CHD4 as a MAP required for MT stabilization and involved in generating spindle bipolarity.

Introduction

The mitotic spindle accurately segregates duplicated chromosomes into daughter cells. Although chromosomes were once considered as passengers in this process, it is now clear that they play a major role in spindle assembly [1, 2], with a key component being the Ran GTPase [3–7]. The RanGTP gradient is produced locally around chromosomes [8]. RanGTP binds to the heterodimeric nuclear transport receptor importin α/β and dissociates nuclear localization signal (NLS)-containing proteins from the importins [9–11]. The liberated NLS proteins play several roles in spindle assembly around chromosomes [12].

We developed a method to isolate NLS proteins from *Xenopus* egg extracts [13] and subsequently purified the microtubule (MT)-associated protein (MAP) fraction [14]. Using the NLS-MAP purification, we identified CHD4 (chromodomain *h*elicase *D*NA binding protein *4*). CHD4 is known as a chromatin-remodeling ATPase and a catalytic subunit of the NuRD (*nu*cleosome-*r*emodeling *d*eacetylase) complex [15]. Although the chromatin-remodeling activity of CHD4 has been established in vitro [16, 17], its function in vivo remains unclear. In flies, germ cells carrying homozygous mutations in CHD4 do not develop [18]. Humans have two orthologs, CHD3 and CHD4. CHD3, but not CHD4, depletion from cultured cells induces prometaphase-like spindle defects [19].

Here, we report that CHD4 is a RanGTP-regulated MAP that localizes to spindle MTs and is essential for spindle assembly. This function of CHD4 involves the RanGTP-dependent stabilization of MTs and organization of MTs into bipolar spindles.

Results

CHD4 Is a Novel MAP that Largely Dissociates from Mitotic Chromatin and Partially Localizes to the Spindle

To identify new RanGTP-regulated MAPs, we sequentially purified NLS proteins and MAPs from cytostatic factor (CSF)-arrested M phase *Xenopus* egg extracts [14]. Mass spectrometry identified 168 proteins, including known RanGTP-regulated MAPs (ISWI, XCTK2, TPX2, HURP, NuMA, and Xkid; see Table S1 available online). The chromatin-remodeling ATPase CHD4 was identified with high confidence (Table S1) and was examined further.

Recombinant CHD4 bound to Taxol-stabilized MTs in a sedimentation assay, although with moderate affinity (Figure S1A). Binding was inhibited by the importin α/β heterodimer, but inhibition was reversed by RanQ69L (a Ran mutant that mimics RanGTP) (Figure 1A).

We made a specific antibody against CHD4 (Figure 1B) and immunostained nuclei and spindles assembled in *Xenopus* egg extracts. In interphase, CHD4 was on chromatin, while in mitosis, it was at the spindle with some enrichment on spindle poles and chromosomes (Figure 1C). The localization was validated using CHD4-depleted extracts and by staining spindles in the presence of recombinant CHD4 (Figures S1B and S1C). In *Xenopus* XL177 cells, CHD4 localized to the nucleus during interphase, while it was cytoplasmic, but enriched on spindle MTs, during mitosis (Figure 1D).

The levels of CHD4 in egg extracts did not change during the cell cycle (Figure S1D). Reisolation of chromatin from cycling egg extracts showed that while CHD4 bound chromatin in interphase, the majority (~87%) dissociated during mitosis, similarly to the chromatin-remodeling ATPase ISWI (*i*mitation *sw*itch) and in contrast to RCC1 (Figure S1E) [20–22]. Moreover, in the absence of chromatin, CHD4 bound to MTs in interphase as well as in mitosis (Figure S1F).

Thus, during interphase, CHD4 is nuclear and separate from MTs. In mitosis, CHD4 mostly dissociates from chromatin and partially localizes to spindle MTs.

Immunodepletion of CHD4 from Egg Extracts Reduces MT Assembly and Prevents Spindle Formation

To address the role of CHD4 in mitosis, we depleted CHD4 from egg extracts (Figure 2A). Nuclei assembled similarly in

*Correspondence: yokoyama@embl.de (H.Y.), mkoffa@mbg.duth.gr (M.D.K.)

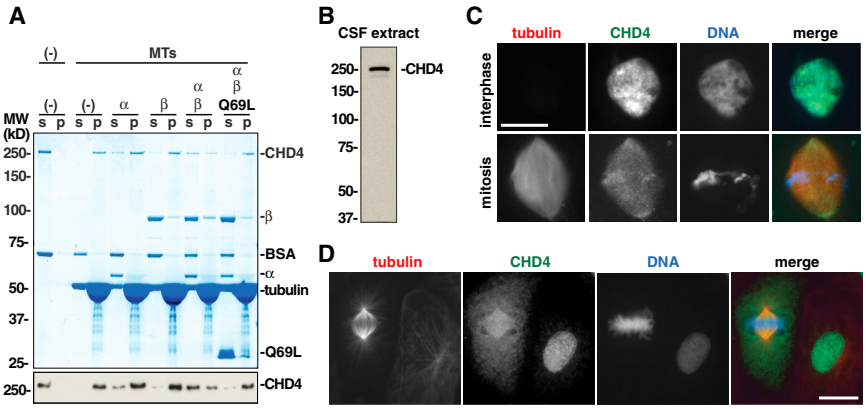

Figure 1. CHD4 Is a RanGTP-Dependent MAP that Dissociates from Mitotic Chromatin and Partially Localizes to the Spindle

(A) Regulation of CHD4 binding to microtubules (MTs) by RanGTP and importin α/β. Recombinant CHD4 (0.20 μM) was incubated with Taxol-stabilized MTs (20 μM) in the presence or absence of 1 μM importin α, 1 μM importin β, and 5 μM RanQ69L. After centrifugation, supernatant (s) and pellet (p) fractions were analyzed by Coomassie staining (top) and immunoblot (bottom). BSA was used as a carrier protein.

(B) Immunoblot of CSF extract with affinity-purified CHD4 antibody.

(C) Localization of CHD4 in *Xenopus* egg extracts. Interphase nuclei and mitotic spindles were assembled and stained with CHD4 antibody and Alexa 488-labeled anti-rabbit IgG (green). Cy3-labeled tubulin is shown in red; DNA stained with Hoechst is blue.

(D) Localization of CHD4 in *Xenopus* XL177 cells. Cells were stained with CHD4 antibody followed by Alexa 488-labeled anti-rabbit IgG (green). Tubulin was stained with anti-tubulin and Alexa 568-labeled anti-mouse IgG (red).

Scale bar represents 20 μm. See also Figure S1.

control and CHD4-depleted interphase extracts (Figure 2B). Ten minutes after inducing mitosis, MTs were generated around chromosomes in control extracts, but not in CHD4-depleted extracts (Figures 2B and 2C). CHD4-depleted extracts eventually nucleated MTs, but these were fewer and did not organize into bipolar spindles (Figures 2B–2D). Chromosomes did not align, and some of them looked detached from the structures (Figure 2B; Figure S2). Addition of recombinant CHD4 to the depleted extracts did not rescue the defects.

Analysis of CHD4 immunoprecipitates from egg extracts identified CHD4 and other NuRD proteins as a stoichiometric complex (Figure 2E). No interaction was detected between CHD4 and other MT-regulating proteins such as XMAP215, EB1, or Cdk11 (Figure 2E). These results suggest that additional NuRD components may affect spindle assembly together with CHD4.

The NuRD Complex Promotes Bipolar Spindle Formation

Bipolar structures can be assembled in the absence of chromatin by adding RanQ69L to egg extracts [3, 5, 7]. Control extracts assembled asters and spindle-like structures after 80 min, ~42% of the structures being bipolar (Figure 3A). CHD4-depleted extracts assembled a similar number of MT structures, but most were asters with fewer MTs (Figures 3A and 3B). Thus, CHD4 affects MT stabilization and bipolarization, but not MT nucleation.

Addition of recombinant CHD4 to the depleted extracts significantly rescued the MT quantity in the RanGTP-induced asters but did not restore bipolarity (Figures 3B and 3C). Addition of the NuRD complex eluted from the CHD4 immunoprecipitates to the depleted extracts fully rescued RanGTP-induced bipolar "spindle" formation (Figure 3C; Figures S3A and S3B; Table S2). The eluted NuRD complex, however, did not rescue sperm spindle assembly (Figure 2). The quality of the complex was possibly inadequate to prevent chromosome scattering at early stages and therefore to rescue chromatin-driven spindle assembly.

CHD4 Is a RanGTP-Dependent MT Stabilizer

We then analyzed whether CHD4 stabilizes MTs in a RanGTP-dependent manner. Incubation of purified centrosomes in control extracts induced MT aster formation, and addition of RanQ69L resulted in increased MT length and density [13]. In CHD4-depleted extracts, centrosomes nucleated asters as in the control, but RanQ69L no longer stabilized MTs (Figure 3D). Addition of either recombinant CHD4 or the NuRD complex to the depleted extracts restored MT stabilization in the presence of RanQ69L (Figure 3E). Importantly, neither CHD4 nor the NuRD complex had an effect on MT stability in the absence of RanQ69L (Figure 3E). Consistently, CHD4 localized to centrosomal asters in a RanGTP-dependent manner (Figures S3C and S3D).

We then examined whether CHD4 stabilizes MTs directly. The MT binding site resides in the N terminus of CHD4, containing an NLS and chromatin-binding domains (PHD and chromodomains) (Figure S4). Recombinant CHD4 and its N-terminal fragment not only bound but also bundled Taxol-stabilized MTs in vitro (Figures 4A and 4B). Bundling was inhibited by the importin α/β heterodimer but reinduced by RanQ69L addition (Figure 4A). Control MTs nucleated with GMPCPP [23] disappeared after treatment on ice for 3 min, while CHD4-induced MT bundles were resistant to depolymerization (Figure 4C). The GFP-CHD4 fusion protein also bundled MTs and bound along the MT length (Figure 4D). The binding was specific, since GFP-CHD4 alone did not aggregate.

The above results (Figures 3 and 4) indicated that CHD4 is responsible for RanGTP-dependent MT stabilization, while the NuRD complex promotes bipolar spindle formation. Neither function requires chromatin remodeling, since they occur in the absence of chromatin.

CHD4 Is Required for Chromosome Alignment in HeLa Cells

Humans encode two orthologs (CHD3 and CHD4) of *Xenopus* CHD4. Human CHD3, but not CHD4, localizes on spindle poles [19]. Depletion of human CHD3 disrupts centrosome integrity and induces spindle defects, while no severe effect was reported for CHD4 [19]. We revisited the role of human CHD4 during mitosis. We confirmed the reported CHD4 localization in the mitotic cytoplasm, but when soluble CHD4 was extracted before fixation, residual CHD4 was found on spindle MTs (Figure S5A).

Three siRNAs targeting CHD4 efficiently silenced CHD4 expression in HeLa cells. Results shown here used siRNA1,

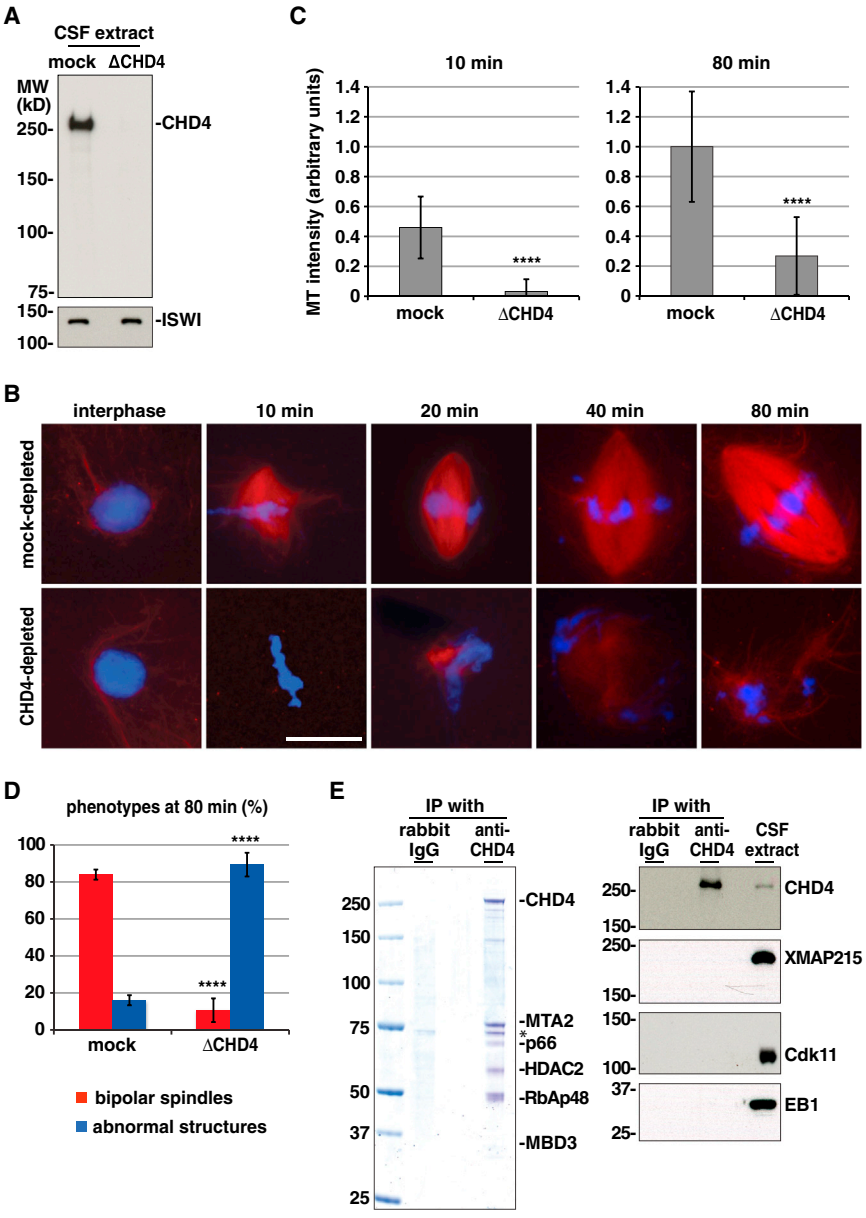

Figure 2. CHD4 Depletion Leads to Severe Spindle Assembly Defects in *Xenopus* Egg Extracts

(A) CSF extract was immunodepleted using rabbit IgG (mock) or anti-CHD4 antibody. Each extract (1 μl) was immunoblotted by the CHD4 antibody and ISWI antibody as a control.

(B) CHD4-depleted extracts neither assemble spindles nor align chromosomes. Mock or CHD4-depleted CSF extracts were supplemented with sperm and Cy3-tubulin (red), driven to interphase, and cycled into mitosis for 80 min. At each time point, aliquots were fixed. DNA was stained with Hoechst (blue). This experiment was reproduced five times. Scale bar represents 20 μm.

(C) CHD4-depleted extracts do not efficiently produce MTs around chromosomes. The MT intensity around sperm assayed in (B) was quantified 10 and 80 min after inducing mitosis. We defined the MT intensity in control extracts after 80 min as 1. n > 30 structures. Error bars represent SD. ****p < 0.0001 (Student's t test, two-tailed).

(D) Quantitation of bipolar spindles assayed in (B). After 80 min, the percentage of bipolar spindles and abnormal MT structures was quantified over the total number of sperm counted. n > 50 sperm heads. Error bars represent SD from four independent experiments. ****p < 0.0001.

(E) The CHD4 antibody specifically immunoprecipitates NuRD complex proteins. CSF extract was incubated with protein A beads covalently coupled to rabbit IgG or the CHD4 antibody. The beads were washed and resuspended in SDS-PAGE sample buffer. Left: the bound proteins were analyzed by Coomassie staining. Proteins in the indicated bands were identified by mass spectrometry. *Hsc70 identified both in control and CHD4 immunoprecipitates. Right: immunoblot against the indicated proteins.

See also Figure S2.

the most efficient (Figure 5A; Figure S5B). Levels of CHD3 and other NuRD components were only slightly affected (Figure 5A). The majority of CHD4-silenced cells (66%) exhibited chromosome alignment defects, categorized as misaligned (one to two chromosomes not aligned at the metaphase plate; 47%) or severe misaligned (more than two chromosomes not aligned; 19%) (Figures 5B and 5C). A small number of cells had lagging chromosomes in anaphase (8%). Control cells also exhibited misaligned chromosomes, but at a much lower frequency (10%) (Figure 5C; Figure S5C).

Live imaging of HeLa cells expressing GFP-α-tubulin and mCherry-H2B showed that control cells formed spindles and divided within 60 min (Figure 5D; Movie S1). CHD4-silenced cells showed significantly prolonged prometaphase (~60 min) as well as metaphase-to-anaphase delay, and their mean division time was 137 min (Figure 5D; Movie S2). Many cells (80 of 150) that initiated anaphase displayed lagging chromosomes.

CHD4-silenced metaphase cells exhibited high levels of BubR1 on kinetochores of unaligned, but also of aligned, chromosomes (Figure 5E). Therefore, in the absence of CHD4, spindle assembly checkpoint signaling on kinetochores is activated, presumably by insufficient tension due to improper MT attachment [24, 25]. Nevertheless, many cells enter anaphase without silencing the BubR1 signal, as previously observed upon HURP or SAF-A depletion [26–28].

Rescue experiments were performed in HeLa cells by sequentially transfecting with control siRNA or CHD4 siRNA1 and a plasmid encoding GFP, wild-type GFP-CHD4, or a siRNA1-resistant mutant GFP-CHD4. Cells were synchronized with nocodazole, released, and arrested in metaphase by the proteasome inhibitor MG132. In the presence of CHD4-siRNA, the mutant GFP-CHD4 protein was expressed, but not the wild-type (Figure 5F, left panel). The expression levels of the mutant GFP-CHD4 were similar to those of endogenous CHD4 (Figure S5D). Chromosome misalignment observed upon CHD4-siRNA was significantly reversed by the mutant GFP-CHD4 (Figure 5F, middle and right panels).

Similarly to HeLa cells, CHD4 is also required for spindle assembly in *Drosophila* cells (called dMi-2). Many (40.3%) dMi-2-depleted mitotic cells exhibited spindle defects, with

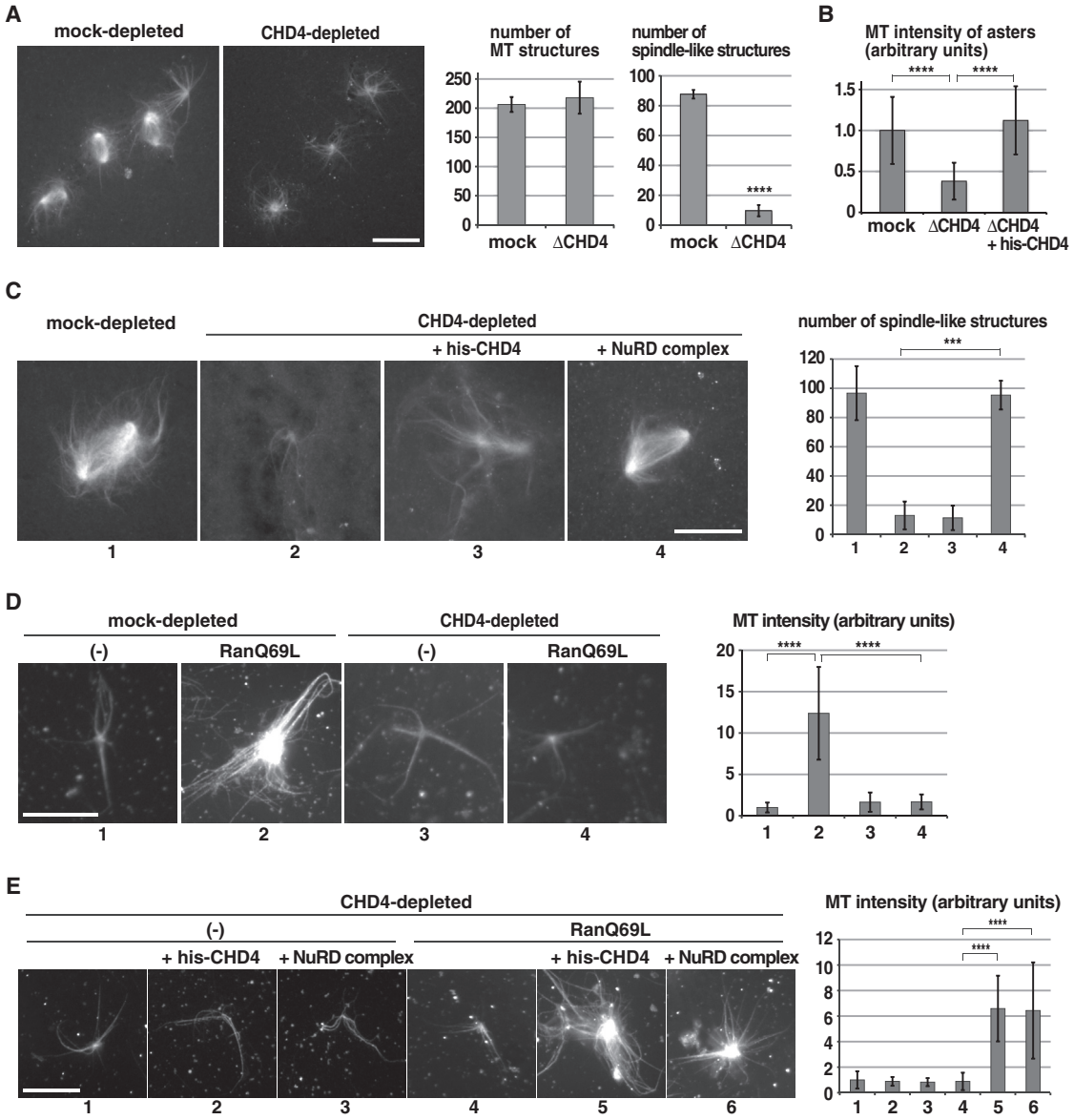

Figure 3. CHD4 Is Required for RanGTP-Dependent MT Stabilization, and NuRD Complex Is Required for Bipolar Spindle Formation

(A) CHD4 depletion does not affect RanGTP-dependent MT nucleation but prevents bipolar spindle formation. Mock and CHD4-depleted CSF extracts were incubated with RanQ69L and Cy3-tubulin at 20°C for 80 min. Numbers of MT structures and spindle-like structures were counted in 100 randomly selected fields with a 63× objective. Error bars represent SD from three independent experiments. ****$p < 0.0001$ (Student's t test, two-tailed).

(B) MT intensity of Ran-induced asters, but not of spindle-like structures, was quantified. $n > 20$ asters. Error bars represent SD. ****$p < 0.0001$.

(C) NuRD complex rescues bipolar spindle formation. The assay shown in (A) was performed in the presence of endogenous CHD4 concentration (0.3 μM) of recombinant CHD4 or purified NuRD complex (Figure S3). Number of spindle-like structures was counted in 100 random fields. Error bars represent SD from three independent experiments. ***$p < 0.001$.

(D) CHD4 depletion prevents RanGTP-dependent MT stabilization. Extracts were incubated with centrosomes, Cy3-tubulin, and anti-TPX2 antibody in the presence or absence of RanQ69L at 20°C for 30 min. The assay was performed in the presence of the TPX2 antibody that inhibits RanGTP-dependent MT nucleation and allows MT nucleation exclusively from centrosomes [13]. MT intensity in centrosomal asters was quantified. $n > 20$ asters. Error bars represent SD. ****$p < 0.0001$.

(E) Recombinant CHD4 rescues RanGTP-dependent MT stabilization. The assay shown in (D) was performed in the presence of recombinant CHD4 or the NuRD complex. $n > 20$ asters. Error bars represent SD. ****$p < 0.0001$.

Scale bars represent 20 μm. See also Figure S3.

few and disorganized MTs (Figures S5E–S5G). Most frequently (19.7%), prometaphase-like defects were found (Figures S5F and S5G). Live-cell imaging of dMi-2-depleted cells showed defective spindles with nonaligned chromosomes, some of which initiated anaphase, causing MT and chromosome segregation defects (Figure S5H; Movies S3, S4, and S5).

CHD4 Is Required for MT Stability and Spindle Assembly in HeLa Cells

CHD4-silenced cells exhibited 20% shorter spindles (8.03 ± 1.00 μm) compared to control cells (10.03 ± 1.07 μm) (Figure 6A), suggesting defects in MT stabilization. We tested whether kinetochore MT stability is affected upon CHD4

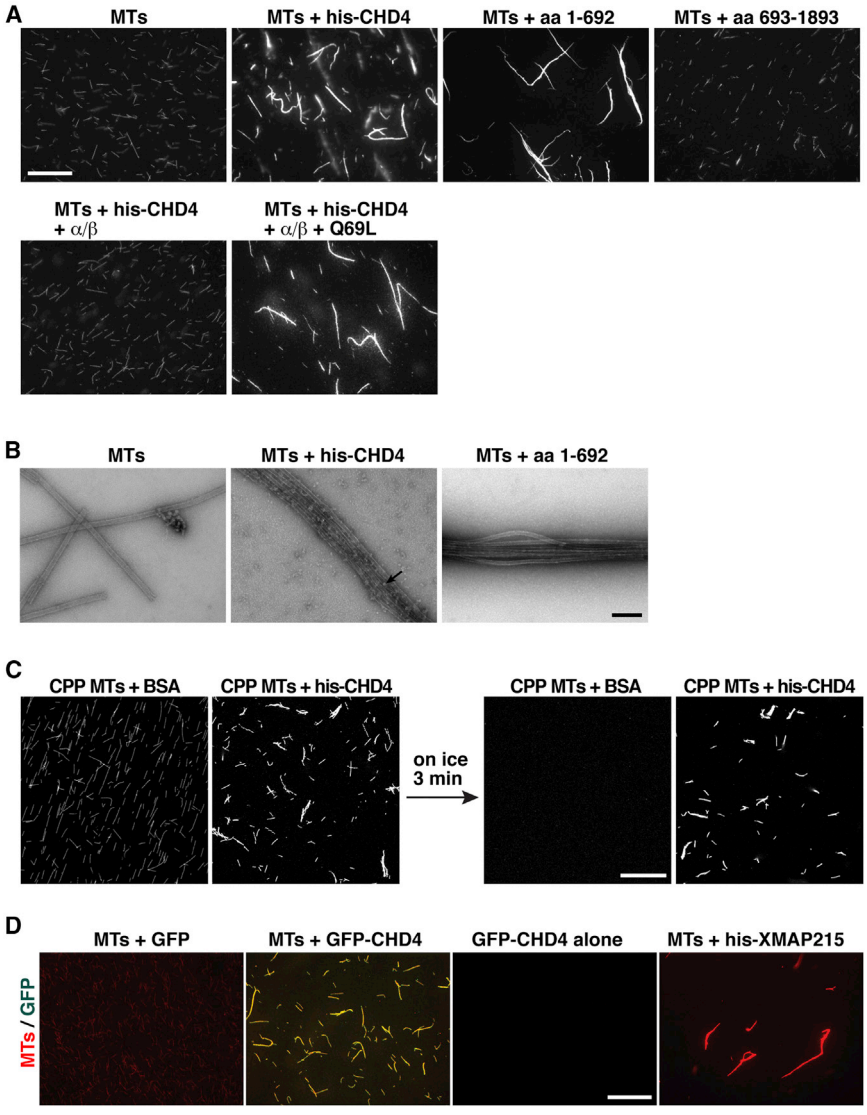

Figure 4. CHD4 Directly Stabilizes MTs in a RanGTP-Dependent Manner

(A) CHD4 bundles MTs in vitro. Recombinant full-length CHD4, aa 1–692, or aa 693–1893 (1 μM) was incubated with 0.3 μM Taxol-stabilized MTs labeled with Cy3 at room temperature (RT) for 10 min. When indicated, 2 μM importin α, 2 μM importin β, or 5 μM RanQ69L was included. Scale bar represents 20 μm.

(B) EM analysis of MT bundles induced by CHD4 in (A) and stained with uranyl acetate. The arrow represents a large protein density. Scale bar represents 0.2 μm.

(C) CHD4 directly stabilizes MTs in vitro. Cy3-labeled GMPCPP MTs were incubated with BSA or his-CHD4 at RT for 10 min. Samples were subsequently incubated on ice for 3 min. Scale bar represents 20 μm.

(D) GFP-CHD4 binds along the MTs in vitro. GFP, GFP-CHD4, or histidine-tagged XMAP215 (1 μM) were incubated with or without Cy3-labeled Taxol-stabilized MTs (0.3 μM) at RT for 10 min. Note that his-XMAP215 is a negative control that bundles MTs but does not show green signals. Scale bar represents 20 μm.

See also Figure S4.

reduction. After cold treatment for 10 min, less-stable MTs depolymerized, but kinetochore fibers were specifically preserved in control cells (Figure 6B) [29]. In CHD4-silenced cells, however, only few kinetochore fibers remained after cold treatment (Figure 6B).

We also examined MT regrowth after longer cold treatment. In control cells, centrosome-nucleated MT asters appeared 45 s after rewarming and were organized into bipolar spindles within 5 min (Figure 6C). In CHD4-silenced cells, two centrosomal asters also appeared, but bipolar spindles formed only after 15–30 min and were often abnormal. MT density was significantly lower in CHD4-silenced cells at early times but recovered later (after 15 min) (Figure 6C).

These results show that CHD4 is required for assembly and stability of kinetochore and centrosomal MTs, regulating overall MT stability in HeLa cells.

Discussion

Physiological Function of CHD4

CHD4 is known as a chromatin-remodeling ATPase and catalytic subunit of the NuRD complex [15]. CHD4 plays important roles in DNA damage response, cell-cycle progression, and transcriptional regulation [30–33]. Here we find that CHD4 is a bona fide MAP. Binding occurs via an N-terminal region containing NLS and chromatin-binding domains and is regulated by RanGTP. In *Xenopus* egg extracts and cultured cells, CHD4 largely dissociates from mitotic chromatin and relocalizes to the mitotic cytoplasm and on the spindle. CHD4 depletion from egg extracts, human cells, or *Drosophila* cells causes MT reduction, chromosome misalignment, and delays in early mitosis, leading to chromosome missegregation in anaphase. The low percentage of mitotic defects reported after human CHD4 depletion [19] may be attributable to differential RNAi efficiencies.

RanGTP-Dependent MT Stabilizers Required for Spindle Assembly

Our in vitro results show that CHD4 is necessary and sufficient for RanGTP-dependent MT stabilization but is not required for MT nucleation. Consistently, CHD4 regulates the stability of both kinetochore and centrosomal MTs in HeLa cells. Cdk11 (*c*yclin-*d*ependent *k*inase 11) is also required for RanGTP-dependent MT stabilization [13], but no interaction was detected between CHD4 and Cdk11. MT stabilization around chromosomes may be distinctly regulated in space: CHD4 could be activated in the vicinity of chromosomes and stabilize MTs there, while substrates phosphorylated by Cdk11 could diffuse and stabilize MTs distant from chromatin.

Chromatin-Remodeling ATPases that Regulate MTs during Mitosis

Among the chromatin-remodeling ATPases [15], our NLS-MAP purification identified only CHD4 and ISWI. Both proteins bind

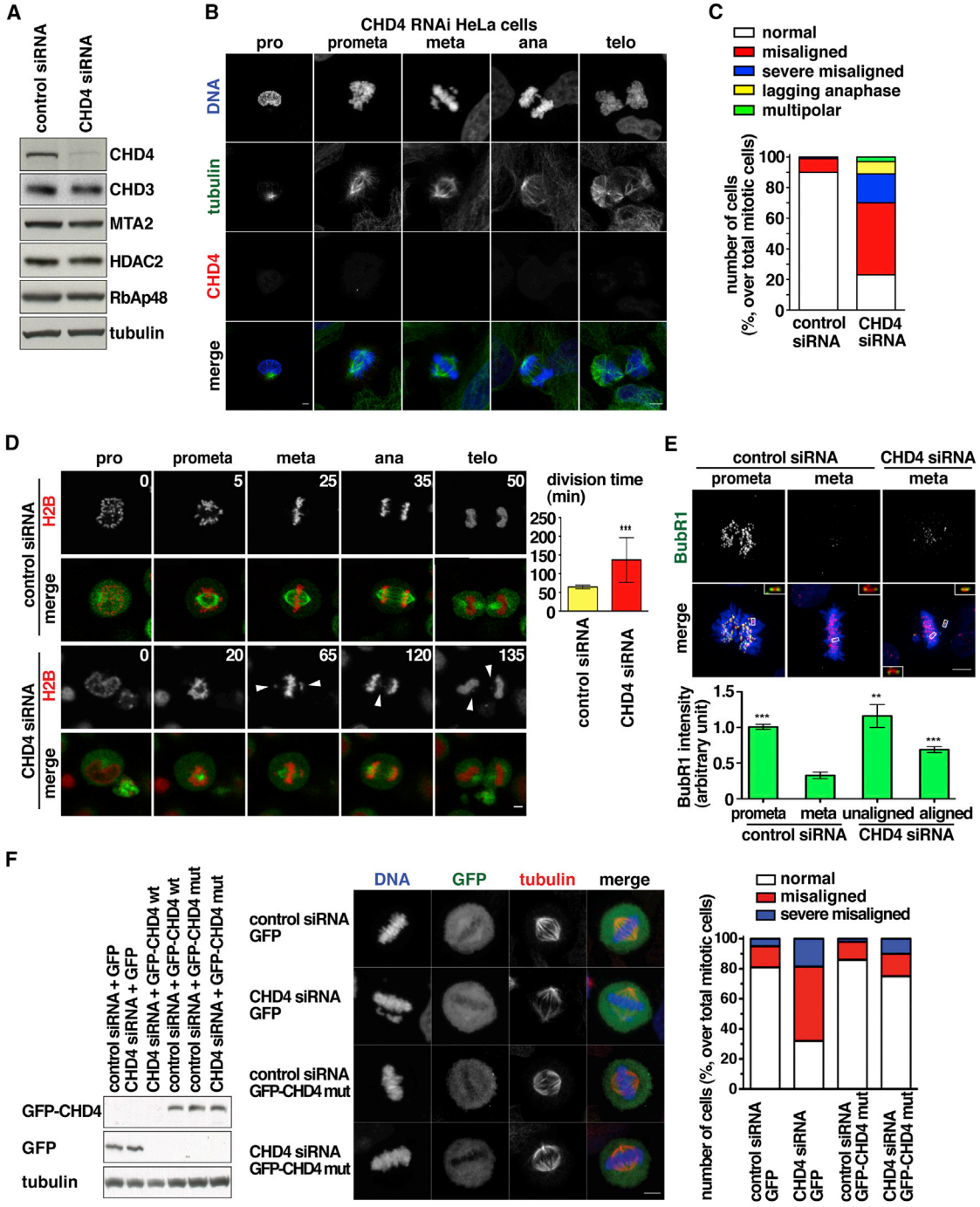

Figure 5. CHD4 Is Required for Chromosome Alignment in Human Cells

(A) Human CHD4 is downregulated by siRNA. HeLa cells were treated with siRNA1 for 48 hr. Whole extracts (10 μg) were immunoblotted.

(B) Mitotic defects associated with CHD4 reduction. 48 hr after siRNA1 treatment, cells were fixed and stained for tubulin (green), CHD4 (red), and DNA (blue). The defects were classified as misaligned, with one to two chromosomes not aligned at the metaphase plate; severe misaligned, with more than two chromosomes not aligned; lagging anaphase, with missegregated chromosomes; and multipolar, with more than two poles.

(C) Quantitation of mitotic defects in cells treated with control siRNA or CHD4 siRNA1 (n = 300 cells from three independent experiments).

(D) Live-cell imaging reveals mitotic delay upon CHD4 reduction. Left: HeLa cells expressing GFP-α-tubulin/H2B-mCherry were imaged after siRNA transfection. Time is presented in minutes. Note that after CHD4 RNAi, we observed unaligned chromosomes at 65 min, lagging chromosomes at 120 min, and micronuclei at 135 min. Control cell, see Movie S1; CHD4-depleted cell, see Movie S2. Right: mitotic division time from prophase to telophase. n ≥ 150 cells from three experiments. ***p < 0.001 (Mann-Whitney test, two-tailed). Error bars represent SD.

(E) CHD4 depletion activates the spindle assembly checkpoint. Top: maximum projections of control or CHD4-depleted HeLa cells stained for BubR1 (green), anti-centromere antibody (ACA, red), and DNA (blue). Insets show a single z slice of boxed regions. Bottom: BubR1 signals were quantified and normalized against ACA signals in control prometaphase or metaphase cells (n = 60 kinetochores) or CHD4-depleted metaphase cells (n = 60 kinetochores of aligned, n = 14 kinetochores of unaligned chromosomes). **p < 0.01, ***p < 0.001. Error bars represent SEM.

(legend continued on next page)

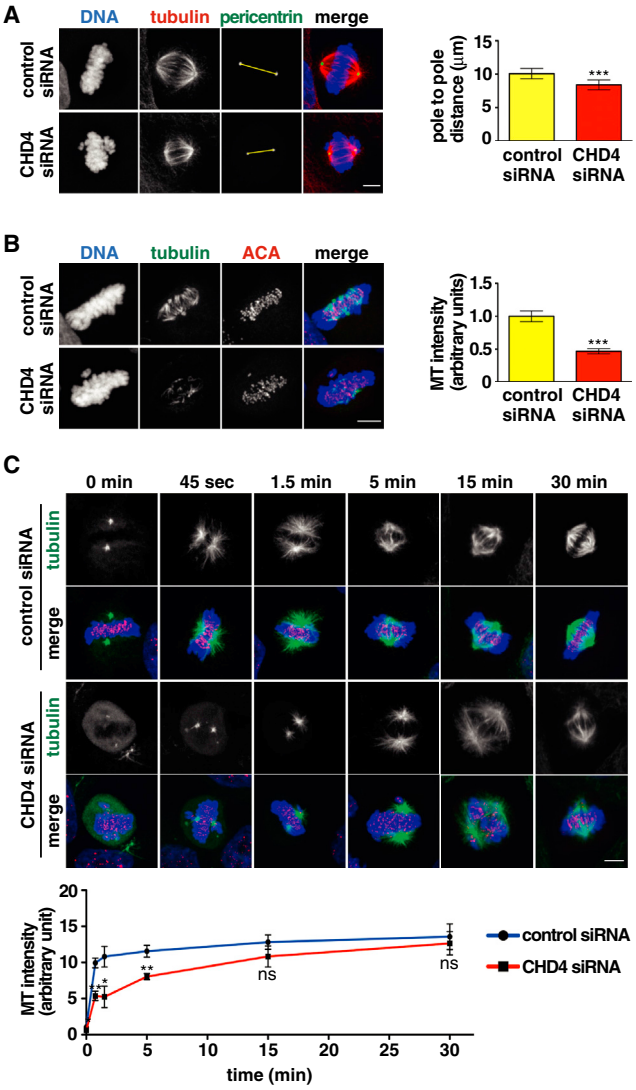

Figure 6. CHD4 Regulates MT Dynamics in HeLa cells

(A) Spindle length is reduced upon CHD4 silencing. Left: maximum projections of control and CHD4 siRNA-treated cells stained for α-tubulin (red), pericentrin (green), and DNA (blue). Yellow lines indicate interpolar distance. Right: interpolar distances measured on single-plane confocal images. n ≥ 60 cells from three independent experiments. ***p < 0.001 (Mann-Whitney test, two-tailed). Error bars represent SD.

(B) CHD4 is required for kinetochore MT stabilization. Left: representative images of cells treated with control or CHD4 siRNA, incubated 10 min on ice, fixed, and stained for α-tubulin (green), ACA (red), and DNA (blue). Right: intensity of kinetochore MTs (n = 60 cells from three experiments). ***p < 0.001. Error bars represent SEM.

(C) CHD4 is required for MT growth from centrosomes. Top: control and CHD4-depleted cells were incubated 1 hr on ice and then rewarmed at 37°C. At the indicated time points, cells were fixed and stained for α-tubulin (green), ACA (red), and DNA (blue). Bottom: MT intensity was quantified (n ≥ 60 cells for each time point, from three independent experiments). ns: p > 0.05, *p < 0.05, **p < 0.01. Error bars represent SEM. Scale bars represent 5 μm.

MTs via NLS and chromatin-binding domains, largely dissociating from mitotic chromatin and relocalizing to the spindle [14, 20, 21]. Their function is temporally distinct, however: CHD4 stabilizes MTs in early mitosis for spindle assembly, while ISWI stabilizes MTs in anaphase for spindle maintenance [14].

The Role of CHD4 and the NuRD Complex in Spindle Assembly

Some NuRD-complex proteins localize to mitotic spindles [19, 34, 35], but the significance of their localization was previously unknown. We find that while CHD4 stabilizes and assembles MTs in a RanGTP-dependent manner, the CHD4-containing NuRD complex promotes their organization into bipolar spindles. These functions of CHD4 and the NuRD complex are independent of chromatin remodeling. Another, HURP-containing, protein complex is also important for maintaining spindle bipolarity in *Xenopus* egg extracts [27]. Whether the HURP-containing and the CHD4-containing NuRD complex regulate MT bipolarization cooperatively or distinctly remains to be determined.

Here, we have uncovered a new role for CHD4 as a MAP in spindle assembly that is essential for chromosome segregation. Interestingly, CHD4 plays an important role in DNA damage repair [30–32]. The two functions of CHD4 are distinct but are both critical in maintaining genome integrity.

Experimental Procedures

Xenopus Egg Extracts and XL177 Cells

CSF-arrested M phase *Xenopus* egg extracts (CSF extracts) were prepared and spindle assembly was performed as described previously [36]. Endogenous CHD4 was depleted from CSF extracts by four rounds of incubation with 60% (vol/vol) Dynabeads protein A coupled with anti-CHD4 antibodies. MT density around sperm was quantified using MATLAB (The MathWorks) [13]. Mass spectrometry of the NLS-MAP fraction purified from CSF extracts, immunofluorescence of egg extracts and XL177 cells, and immunoprecipitation of CHD4 and elution were performed as described in the Supplemental Experimental Procedures.

Recombinant Proteins and Antibodies

A cDNA clone (IMAGE 4683903, RZPD) covering the complete *Xenopus* CHD4 cDNA was subcloned into pFastBac HTa (Invitrogen). Recombinant CHD4 was expressed in Sf21 insect cells and purified on TALON beads (BD Biosciences), Mono Q, and Mono S columns (GE). GFP-CHD4 and aa 693–1893 were similarly prepared. aa 1–692 was expressed in bacteria and purified by TALON, Mono Q, and Mono S. Importin α, importin β, and RanQ69L-GTP were prepared as described previously [13]. A rabbit polyclonal antibody against *Xenopus* CHD4 was prepared and purified against recombinant CHD4.

MT Assays In Vitro and in Egg Extracts

MT sedimentation and MT bundling assays are described in the Supplemental Experimental Procedures. A RanGTP-dependent MT nucleation assay [3] and a RanGTP-dependent MT stabilization assay [13] were performed as described previously. Recombinant CHD4 or purified NuRD complex was added back to the CHD4-depleted CSF extracts in a quantity corresponding to endogenous CHD4 (0.3 μM). The density of MT asters was quantified using MATLAB [13].

Chromatin Isolation

CSF extracts were supplemented with sperm nuclei and Cy3-tubulin, driven into interphase, and cycled into mitosis. At each time point, an aliquot was taken and chromatin was isolated by centrifugation [21].

(F) Rescue of the CHD4 siRNA-induced phenotype. HeLa cells were sequentially transfected with control siRNA or CHD4 siRNA1 and a plasmid encoding GFP, GFP-CHD4 wild-type (wt), or GFP-CHD4 siRNA1-resistant mutant (mut). Cells were arrested in metaphase by MG132. Left: western blot of cell extracts with GFP and α-tubulin antibodies. Middle: maximum projections of cells stained for tubulin (red) and DNA (blue). GFP or GFP-CHD4 mut is green. Right: the percentage of normal, misaligned, and severe misaligned phenotypes in cells transfected as indicated. n = 200 cells from two independent experiments. Scale bars represent 5 μm. See also Figure S5.

Drosophila S2 Cells

RNAi was performed as described previously [37]. dMi-2 dsRNAs (63697 and HFA11222) were prepared according to the GenomeRNAi database [38]. Immunoblotting, immunofluorescence, and live imaging were performed as described in the Supplemental Experimental Procedures.

HeLa Cells

siRNA oligonucleotides for CHD4 were obtained from Ambion: (1) 5′-CCCA GAAGAGGAUUUGUCATT-3′, (2) 5′-GGUUUAAGCUCUUAGAACATT-3′, and (3) 5′-GGAGCGUAUGCUCUUAUGCTT-3′. Western blotting, immunofluorescence, live imaging, rescue experiments, and MT assays were performed as described in the Supplemental Experimental Procedures.

Supplemental Information

Supplemental Information includes five figures, two tables, Supplemental Experimental Procedures, and five movies and can be found with this article online at http://dx.doi.org/10.1016/j.cub.2013.09.062.

Acknowledgments

We thank A. Brehm for dMi-2 antibody, A. Perez-Gonzalez for FACS analysis, H. Maiato for S2 GFP-α-tubulin/centromere identifier-mCherry cells, J. Ellenberg for HeLa GFP-α-tubulin/H2B-mCherry cells, H. van Attikum for a plasmid encoding human CHD4, K. Crnokic for the frogs, and members of the Mattaj lab for discussions. We also thank the Advanced Light Microscopy, Protein Expression and Purification Core, and Proteomics Core Facilities at EMBL, as well as the CIBIT microscopy facility at the Department of Molecular Biology and Genetics, DUTH. K.N. was supported by IKYDA, P-CUBE short-term fellowships, and ERANetRUS.

Received: January 31, 2013
Revised: August 19, 2013
Accepted: September 30, 2013
Published: November 21, 2013

References

1. Karsenti, E., Newport, J., Hubble, R., and Kirschner, M. (1984). Interconversion of metaphase and interphase microtubule arrays, as studied by the injection of centrosomes and nuclei into Xenopus eggs. J. Cell Biol. *98*, 1730–1745.
2. Heald, R., Tournebize, R., Blank, T., Sandaltzopoulos, R., Becker, P., Hyman, A., and Karsenti, E. (1996). Self-organization of microtubules into bipolar spindles around artificial chromosomes in Xenopus egg extracts. Nature *382*, 420–425.
3. Carazo-Salas, R.E., Guarguaglini, G., Gruss, O.J., Segref, A., Karsenti, E., and Mattaj, I.W. (1999). Generation of GTP-bound Ran by RCC1 is required for chromatin-induced mitotic spindle formation. Nature *400*, 178–181.
4. Zhang, C., Hughes, M., and Clarke, P.R. (1999). Ran-GTP stabilises microtubule asters and inhibits nuclear assembly in Xenopus egg extracts. J. Cell Sci. *112*, 2453–2461.
5. Kalab, P., Pu, R.T., and Dasso, M. (1999). The ran GTPase regulates mitotic spindle assembly. Curr. Biol. *9*, 481–484.
6. Ohba, T., Nakamura, M., Nishitani, H., and Nishimoto, T. (1999). Self-organization of microtubule asters induced in Xenopus egg extracts by GTP-bound Ran. Science *284*, 1356–1358.
7. Wilde, A., and Zheng, Y. (1999). Stimulation of microtubule aster formation and spindle assembly by the small GTPase Ran. Science *284*, 1359–1362.
8. Kalab, P., Weis, K., and Heald, R. (2002). Visualization of a Ran-GTP gradient in interphase and mitotic Xenopus egg extracts. Science *295*, 2452–2456.
9. Gruss, O.J., Carazo-Salas, R.E., Schatz, C.A., Guarguaglini, G., Kast, J., Wilm, M., Le Bot, N., Vernos, I., Karsenti, E., and Mattaj, I.W. (2001). Ran induces spindle assembly by reversing the inhibitory effect of importin alpha on TPX2 activity. Cell *104*, 83–93.
10. Nachury, M.V., Maresca, T.J., Salmon, W.C., Waterman-Storer, C.M., Heald, R., and Weis, K. (2001). Importin beta is a mitotic target of the small GTPase Ran in spindle assembly. Cell *104*, 95–106.
11. Wiese, C., Wilde, A., Moore, M.S., Adam, S.A., Merdes, A., and Zheng, Y. (2001). Role of importin-beta in coupling Ran to downstream targets in microtubule assembly. Science *291*, 653–656.
12. Meunier, S., and Vernos, I. (2012). Microtubule assembly during mitosis - from distinct origins to distinct functions? J. Cell Sci. *125*, 2805–2814.
13. Yokoyama, H., Gruss, O.J., Rybina, S., Caudron, M., Schelder, M., Wilm, M., Mattaj, I.W., and Karsenti, E. (2008). Cdk11 is a RanGTP-dependent microtubule stabilization factor that regulates spindle assembly rate. J. Cell Biol. *180*, 867–875.
14. Yokoyama, H., Rybina, S., Santarella-Mellwig, R., Mattaj, I.W., and Karsenti, E. (2009). ISWI is a RanGTP-dependent MAP required for chromosome segregation. J. Cell Biol. *187*, 813–829.
15. Clapier, C.R., and Cairns, B.R. (2009). The biology of chromatin remodeling complexes. Annu. Rev. Biochem. *78*, 273–304.
16. Brehm, A., Längst, G., Kehle, J., Clapier, C.R., Imhof, A., Eberharter, A., Müller, J., and Becker, P.B. (2000). dMi-2 and ISWI chromatin remodelling factors have distinct nucleosome binding and mobilization properties. EMBO J. *19*, 4332–4341.
17. Wang, H.B., and Zhang, Y. (2001). Mi2, an auto-antigen for dermatomyositis, is an ATP-dependent nucleosome remodeling factor. Nucleic Acids Res. *29*, 2517–2521.
18. Kehle, J., Beuchle, D., Treuheit, S., Christen, B., Kennison, J.A., Bienz, M., and Müller, J. (1998). dMi-2, a hunchback-interacting protein that functions in polycomb repression. Science *282*, 1897–1900.
19. Sillibourne, J.E., Delaval, B., Redick, S., Sinha, M., and Doxsey, S.J. (2007). Chromatin remodeling proteins interact with pericentrin to regulate centrosome integrity. Mol. Biol. Cell *18*, 3667–3680.
20. MacCallum, D.E., Losada, A., Kobayashi, R., and Hirano, T. (2002). ISWI remodeling complexes in Xenopus egg extracts: identification as major chromosomal components that are regulated by INCENP-aurora B. Mol. Biol. Cell *13*, 25–39.
21. Demeret, C., Bocquet, S., Lemaître, J.M., Françon, P., and Méchali, M. (2002). Expression of ISWI and its binding to chromatin during the cell cycle and early development. J. Struct. Biol. *140*, 57–66.
22. Li, H.Y., and Zheng, Y. (2004). Phosphorylation of RCC1 in mitosis is essential for producing a high RanGTP concentration on chromosomes and for spindle assembly in mammalian cells. Genes Dev. *18*, 512–527.
23. Hyman, A.A., Salser, S., Drechsel, D.N., Unwin, N., and Mitchison, T.J. (1992). Role of GTP hydrolysis in microtubule dynamics: information from a slowly hydrolyzable analogue, GMPCPP. Mol. Biol. Cell *3*, 1155–1167.
24. Skoufias, D.A., Andreassen, P.R., Lacroix, F.B., Wilson, L., and Margolis, R.L. (2001). Mammalian mad2 and bub1/bubR1 recognize distinct spindle-attachment and kinetochore-tension checkpoints. Proc. Natl. Acad. Sci. USA *98*, 4492–4497.
25. Chan, G.K., Jablonski, S.A., Sudakin, V., Hittle, J.C., and Yen, T.J. (1999). Human BUBR1 is a mitotic checkpoint kinase that monitors CENP-E functions at kinetochores and binds the cyclosome/APC. J. Cell Biol. *146*, 941–954.
26. Wong, J., and Fang, G. (2006). HURP controls spindle dynamics to promote proper interkinetochore tension and efficient kinetochore capture. J. Cell Biol. *173*, 879–891.
27. Koffa, M.D., Casanova, C.M., Santarella, R., Köcher, T., Wilm, M., and Mattaj, I.W. (2006). HURP is part of a Ran-dependent complex involved in spindle formation. Curr. Biol. *16*, 743–754.
28. Ma, N., Matsunaga, S., Morimoto, A., Sakashita, G., Urano, T., Uchiyama, S., and Fukui, K. (2011). The nuclear scaffold protein SAF-A is required for kinetochore-microtubule attachment and contributes to the targeting of Aurora-A to mitotic spindles. J. Cell Sci. *124*, 394–404.
29. Rieder, C.L. (1981). The structure of the cold-stable kinetochore fiber in metaphase PtK1 cells. Chromosoma *84*, 145–158.
30. Larsen, D.H., Poinsignon, C., Gudjonsson, T., Dinant, C., Payne, M.R., Hari, F.J., Rendtlew Danielsen, J.M., Menard, P., Sand, J.C., Stucki, M., et al. (2010). The chromatin-remodeling factor CHD4 coordinates signaling and repair after DNA damage. J. Cell Biol. *190*, 731–740.
31. Polo, S.E., Kaidi, A., Baskcomb, L., Galanty, Y., and Jackson, S.P. (2010). Regulation of DNA-damage responses and cell-cycle progression by the chromatin remodelling factor CHD4. EMBO J. *29*, 3130–3139.
32. Smeenk, G., Wiegant, W.W., Vrolijk, H., Solari, A.P., Pastink, A., and van Attikum, H. (2010). The NuRD chromatin-remodeling complex regulates signaling and repair of DNA damage. J. Cell Biol. *190*, 741–749.
33. O'Shaughnessy, A., and Hendrich, B. (2013). CHD4 in the DNA-damage response and cell cycle progression: not so NuRDy now. Biochem. Soc. Trans. *41*, 777–782.

34. Chadwick, B.P., and Willard, H.F. (2002). Cell cycle-dependent localization of macroH2A in chromatin of the inactive X chromosome. J. Cell Biol. *157*, 1113–1123.
35. Sakai, H., Urano, T., Ookata, K., Kim, M.H., Hirai, Y., Saito, M., Nojima, Y., and Ishikawa, F. (2002). MBD3 and HDAC1, two components of the NuRD complex, are localized at Aurora-A-positive centrosomes in M phase. J. Biol. Chem. *277*, 48714–48723.
36. Hannak, E., and Heald, R. (2006). Investigating mitotic spindle assembly and function in vitro using Xenopus laevis egg extracts. Nat. Protoc. *1*, 2305–2314.
37. Bettencourt-Dias, M., and Goshima, G. (2009). RNAi in Drosophila S2 cells as a tool for studying cell cycle progression. Methods Mol. Biol. *545*, 39–62.
38. Horn, T., Arziman, Z., Berger, J., and Boutros, M. (2007). GenomeRNAi: a database for cell-based RNAi phenotypes. Nucleic Acids Res. *35* (Database issue), D492–D497.